

# Theoretical Expression of the Average Activation–Deactivation Equilibrium Constant in Controlled/Living Free-Radical Copolymerization Operating via Reversible Termination. Application to a Strongly Improved Control in Nitroxide-Mediated Polymerization of Methyl Methacrylate

Bernadette Charleux,<sup>\*,†</sup> Julien Nicolas,<sup>†</sup> and Olivier Guerret<sup>‡</sup>

Laboratoire de Chimie des Polymères, UMR 7610 associée au CNRS, Université Pierre et Marie Curie, T44 E1, 4 Place Jussieu, 75252 Paris Cedex 05, France, and ARKEMA, Groupement de Recherches de Lacq, B.P. No. 34, 64170 LACQ, France

Received January 14, 2005; Revised Manuscript Received April 25, 2005

**ABSTRACT:** The average activation–deactivation equilibrium constant,  $\langle K \rangle$ , was determined on a theoretical basis for controlled free-radical copolymerizations operating via a reversible termination mechanism (i.e., nitroxide-mediated polymerization or atom transfer radical polymerization), using the terminal model for the activation–deactivation equilibrium and the terminal model or the implicit penultimate unit effect model for the propagation reaction. From the equation, it was shown that the addition of a small fraction of an appropriate comonomer to a monomer with a very large activation–deactivation equilibrium constant,  $K$ , might lead to strong reduction of  $\langle K \rangle$ , providing the added comonomer exhibits a low  $K$ . In nitroxide-mediated polymerization, the monomers with a very high  $K$ , such as the methacrylic esters, do not lead to controlled polymerization in the presence of nitroxides like SG1, despite the absence of disproportionation reaction between the nitroxide and the growing radical, because of the too fast irreversible self-termination of the propagating radicals present in high concentration. The polymerization stops at low conversion. Consequently, a reduction of  $K$  might lead to an enhanced quality of control. The method was indeed successfully applied to the SG1-mediated polymerization of methyl methacrylate at 90 °C. By adding only 4.4 or 8.8 mol % of styrene, the polymerization could be carried out to large conversions, while exhibiting all the features of a controlled system.

## Introduction

Controlled/living free radical polymerization (CRP)<sup>1</sup> via a reversible termination mechanism consists of two main techniques, i.e., nitroxide-mediated polymerization (NMP)<sup>2</sup> and atom transfer radical polymerization (ATRP).<sup>3,4</sup> Both are based on an activation–deactivation equilibrium between dominant dormant species and a small fraction of propagating macroradicals. The involved mechanisms are now well established for both methods, and the kinetic and thermodynamic parameters have been determined for the homopolymerization of the most common monomers. NMP and ATRP have also been applied to the synthesis of statistical copolymers, revealing a composition gradient when the comonomers exhibit a noticeable difference in reactivity.<sup>2–11</sup> However, to our knowledge, despite the opportunity of creating new architectures, the kinetics and thermodynamics of controlled/living statistical copolymerization have not been so largely investigated as those of homopolymerization.<sup>5,10,12–15</sup> In a first approach, the reactivity ratios have been studied to compare their values with those of a conventional radical copolymerization. Similar values are actually expected since they correspond to the intrinsic reactivity of the involved macroradicals and monomers. It is indeed generally shown that the reactivity ratios determined in a controlled/living radical copolymerization proceeding via an activation–deactivation mechanism of the growing mac-

roradicals do not strongly differ from those measured in the analogous conventional free-radical copolymerization, meaning that the composition equation is the same.<sup>5,10,16</sup> However, some deviation can be found, especially when the traditional methods to measure the reactivity ratios are applied, i.e., analysis of the copolymer composition at low monomer conversion for short chains. This is explained by the inadequacy of the general assumptions made in the Mayo–Lewis approach, which are only valid for long-chain copolymerizations. Only the methods using integrated composition equations, such as the Skeist equation,<sup>17</sup> are applicable. The influence of the short-chain radicals reactivity, which differs from that of the long-chain macroradicals, has been first discussed.<sup>11,18</sup> In addition, establishment of both the activation–deactivation equilibrium and the cross-propagation equilibrium (steady-state assumption for the concentration of all propagating macroradicals) might require a certain time, i.e., a certain monomer conversion. As proposed by Matyjaszewski for ATRP systems,<sup>19</sup> the deviation is better explained by a slow establishment of the cross-propagation equilibrium. The same conclusion was also illustrated by Klumperman et al.<sup>18</sup> in the simulated atom transfer radical copolymerization of styrene and *n*-butyl acrylate, where 15% overall monomer conversion was needed to reach the steady-state concentrations in propagating radicals. When the cross-propagation rates are equal, copolymers from both conventional and living free-radical copolymerizations should exhibit the same instantaneous composition. In contrast, even though the ratio of the macroradicals concentration does not differ for both

<sup>†</sup> Université Pierre et Marie Curie.

<sup>‡</sup> ARKEMA.

\* Corresponding author: e-mail charleux@ccr.jussieu.fr.

methods, there is no reason to have the same overall radicals concentration and hence the same copolymerization rate.<sup>5</sup> This last point has not been thoroughly discussed in the literature and should be addressed.

In this article, we present a theoretical approach to describe the copolymerization kinetics in controlled/living copolymerization operating via reversible termination. Both the average activation–deactivation equilibrium constant  $\langle K \rangle$  and the product with the average rate constant of propagation,  $\langle k_p \rangle \langle K \rangle$ , are determined on a fully theoretical basis. The model is developed for nitroxide-mediated polymerization but might be easily extended to ATRP. The terminal model (TM) and the implicit penultimate unit effect model (IPUE) have been considered for the propagation reaction. In contrast, the activation–deactivation equilibrium constant was supposed to depend on the terminal monomer unit only. This last point has been discussed by Heuts et al.,<sup>13</sup> who concluded that such an assumption was quite reasonable, even though not experimentally proven. In their work, these authors<sup>13</sup> had already proposed an equation for  $\langle K \rangle$  in an ATRP system as a function of the individual equilibrium constants and of the ratio of the propagating radicals concentration. Here, we go a step further in presenting  $\langle K \rangle$  as a simple function of the comonomer feed ratio and of known kinetic and thermodynamic parameters, for both the terminal model and the IPUE model.

The variation of  $\langle K \rangle$  and  $\langle k_p \rangle \langle K \rangle$  with the comonomer composition is discussed and further applied to the nitroxide-mediated copolymerization of methyl methacrylate and styrene, where it is shown that a small fraction of styrene can have a remarkable influence. This experimental application will be presented in the second part of the article.

### Theoretical Approach of the Average Activation–Deactivation Equilibrium Constant

We consider two monomers A and B. The free nitroxide is noted N, and the macromolecular alkoxyamines are respectively A–N and B–N, where A and B represent the last monomer unit.

The average activation–deactivation equilibrium constant reads

$$\langle K \rangle = \frac{[P^*][N]}{[P-N]} = \frac{[P^*][N]}{C_0} \quad (1)$$

where  $[P^*] = [A^*] + [B^*]$  is the overall concentration of propagating radicals, with  $[A^*]$  the concentration of A-terminated macroradicals and  $[B^*]$  the concentration of B-terminated macroradicals.  $[P-N]$  is the overall alkoxyamine concentration, which is considered to match the initial alkoxyamine concentration,  $C_0 = [P-N] = [A-N] + [B-N]$ .

The activation–deactivation equilibrium constant,  $K_A$ , in the N-mediated polymerization of A, is related to  $[A^*]$  and to the concentration of A-terminated dormant chains  $[A-N]$  according to eq 2; the same relationship also holds for  $K_B$  (eq 3).

$$K_A = \frac{[A^*][N]}{[A-N]} \quad (2)$$

$$K_B = \frac{[B^*][N]}{[B-N]} \quad (3)$$

The overall concentration of propagating radicals is then given by eq 4, and combination with eq 1 allows to write the average equilibrium constant as in eq 5.

$$[P^*] = K_A \frac{[A-N]}{[N]} + K_B \frac{[B-N]}{[N]} \quad (4)$$

$$\langle K \rangle = K_A \frac{[A-N]}{C_0} + K_B \frac{[B-N]}{C_0} \quad (5)$$

The rate of copolymerization,  $R_p$ , depends on the overall concentration of propagating macroradicals according to the following eq 6, where conv represents the overall molar conversion.

$$R_p = -\frac{d([A] + [B])}{dt} = \langle k_p \rangle [P^*]([A] + [B]) \quad (6)$$

$$\frac{d[\ln(1/(1 - \text{conv}))]}{dt} = \langle k_p \rangle [P^*] = \langle k_p \rangle \langle K \rangle \frac{C_0}{[N]} \quad (7)$$

The slope of the usual  $\ln[1/(1 - \text{conv})]$  vs time plot is a direct function of  $\langle k_p \rangle \langle K \rangle$ . Like in homopolymerization, it also depends on the concentrations of both the alkoxyamine initiator and the nitroxide. The latter continuously increases throughout the polymerization owing to the so-called persistent radical effect, resulting from the irreversible self-termination of the propagating macroradicals.<sup>20</sup> However, when a sufficiently high concentration of free nitroxide is initially introduced, the concentration  $[N]$  might remain close to the initial one; i.e., the kinetics depends in that case on the initial  $C_0/[N]_0$  ratio.<sup>21</sup>

**1. Terminal Model for Propagation.** Only the two chain ends  $A^*$  and  $B^*$  are considered. When it applies, the cross-propagation equilibrium allows to write

$$k_{BA}[B^*][A] = k_{AB}[A^*][B] \quad (8)$$

where  $k_{BA}$  and  $k_{AB}$  are the cross-propagation rate constants.

With the reactivity ratios  $r_A = k_{AA}/k_{AB}$  and  $r_B = k_{BB}/k_{BA}$  ( $k_{AA}$  and  $k_{BB}$  are the homopropagation rate constants, also noted  $k_{p,A}$  and  $k_{p,B}$ ), this relationship gives

$$\frac{[A^*]}{[B^*]} = \frac{r_A k_{p,B}}{r_B k_{p,A}} \frac{[A]}{[B]} = \frac{r_A k_{p,B} f_A}{r_B k_{p,A} f_B} \quad (9)$$

where  $f_A$  and  $f_B$  are the molar fraction of A and B, respectively, in the comonomer mixture.

From the activation–deactivation equilibria (eqs 2 and 3), the ratio of the propagating macroradicals concentrations also reads as in eq 10, which leads to the ratio of the dormant species concentrations (eq 11), when combined with eq 9.

$$\frac{[A^*]}{[B^*]} = \frac{K_A}{K_B} \frac{[A-N]}{[B-N]} \quad (10)$$

$$\frac{[A-N]}{[B-N]} = \frac{K_B}{K_A} \frac{r_A k_{p,B} f_A}{r_B k_{p,A} f_B} \quad (11)$$

With  $C_0 = [A-N] + [B-N]$ , the proportion of each individual type of dormant chain can be calculated as in eqs 12 and 13.

$$\frac{[A-N]}{C_0} = \frac{K_B r_A k_{p,B} f_A}{K_A r_B k_{p,A} f_B + K_B r_A k_{p,B} f_A} \quad (12)$$

$$\frac{[B-N]}{C_0} = \frac{K_A r_B k_{p,A} f_B}{K_A r_B k_{p,A} f_B + K_B r_A k_{p,B} f_A} \quad (13)$$

The average activation–deactivation equilibrium constant of eq 5 is then given by the following relationships (eqs 14 and 15).

$$\langle K \rangle = \frac{K_A K_B r_A k_{p,B} f_A + K_B K_A r_B k_{p,A} f_B}{K_A r_B k_{p,A} f_B + K_B r_A k_{p,B} f_A} \quad (14)$$

$$\langle K \rangle = \frac{\frac{r_A f_A}{k_{p,A}} + \frac{r_B f_B}{k_{p,B}}}{\frac{r_A f_A}{k_{p,A} K_A} + \frac{r_B f_B}{k_{p,B} K_B}} \quad (15)$$

It appears that  $\langle K \rangle$  not only depends on the individual equilibrium constants and the comonomer composition but also is affected by the cross-propagation rate constants (actually represented by  $k_p$ /reactivity ratio).

With  $\langle k_p \rangle$  given by the terminal model (eq 16),<sup>22–24</sup> it is possible to calculate the  $\langle k_p \rangle \langle K \rangle$  product as follows:

$$\langle k_p \rangle = \frac{r_A f_A^2 + 2f_A f_B + r_B f_B^2}{r_A \frac{f_A}{k_{p,A}} + r_B \frac{f_B}{k_{p,B}}} \quad (16)$$

$$\langle k_p \rangle \langle K \rangle = \frac{r_A f_A^2 + 2f_A f_B + r_B f_B^2}{\frac{r_A f_A}{k_{p,A} K_A} + \frac{r_B f_B}{k_{p,B} K_B}} \quad (17)$$

**2. Implicit Penultimate Unit Effect for Propagation.** We consider here the IPUE for the propagation and cross-propagation reactions. This leads to the existence of four different types of propagating macro-radicals noted  $AA^*$ ,  $AB^*$ ,  $BB^*$ , and  $BA^*$  and of four reactivity ratios:<sup>5,23,24</sup>

$$\text{two monomer reactivity ratios: } r_A = \frac{k_{AAA}}{k_{AAB}} = \frac{k_{BAA}}{k_{BAB}} \text{ and } r_B = \frac{k_{ABB}}{k_{ABA}} = \frac{k_{BBB}}{k_{BBA}}$$

$$\text{two radical reactivity ratios: } s_A = \frac{k_{BAA}}{k_{AAA}} \text{ and } s_B = \frac{k_{ABB}}{k_{BBB}}$$

where  $k_{AAA} = k_{p,A}$  and  $k_{BBB} = k_{p,B}$  are the homopropagation rate constants, and the other rate constants correspond to the different propagation reactions.

In contrast, like before, we consider only two activation–deactivation equilibrium constants,  $K_A$  and  $K_B$ ; i.e., we assume the absence of the penultimate unit effect for  $K$ . Therefore, all the equations from (1) to (7) remain the same, with  $[A^*] = [AA^*] + [BA^*]$  and  $[B^*] = [BB^*] + [AB^*]$ .

When they apply, the cross-propagation equilibria allow to write the concentration ratios given in eqs 18–20.

$$\frac{[AA^*]}{[AA^*] + [BA^*]} = \frac{r_A f_A}{r_A f_A + f_B/s_A} \quad (18)$$

$$\frac{[BB^*]}{[BB^*] + [AB^*]} = \frac{r_B f_B}{r_B f_B + f_A/s_B} \quad (19)$$

$$\frac{[BA^*]}{[AB^*]} = \left( \frac{f_A + r_B f_B}{r_A f_A + f_B} \right) \left( \frac{s_B k_{BBB}/r_B}{s_A k_{AAA}/r_A} \right) \quad (20)$$

The activation–deactivation equilibria in eqs 2 and 3 give relationship 21, which can also be written as in eq 22.

$$\frac{[A^*]}{[B^*]} = \frac{K_A [A-N]}{K_B [B-N]} \quad (21)$$

$$\frac{[A^*]}{[B^*]} = \frac{[AA^*] + [BA^*]}{[BB^*] + [AB^*]} \quad (22)$$

After combination with the previous eqs 18–20, the radical concentration ratio can be expressed by the eq 23.

$$\frac{[A^*]}{[B^*]} = \left( \frac{r_A f_A + f_B/s_A}{r_A f_A + f_B} \right) \left( \frac{r_B f_B + f_A}{r_B f_B + f_A/s_B} \right) \frac{f_A k_{p,B} r_A}{f_B k_{p,A} r_B} \quad (23)$$

With the usual notation given below

$$\overline{k_{p,A}} = k_{p,A} \frac{r_A f_A + f_B}{r_A f_A + f_B/s_A} \quad (24)$$

$$\overline{k_{p,B}} = k_{p,B} \frac{r_B f_B + f_A}{r_B f_B + f_A/s_B} \quad (25)$$

one can simplify the eq 23 in the following manner (eq 26).

$$\frac{[A^*]}{[B^*]} = \frac{r_A \overline{k_{p,B}} f_A}{r_B \overline{k_{p,A}} f_B} \quad (26)$$

In combining eq 21 with eq 26 and considering  $C_0 = [A-N] + [B-N]$ , the ratios  $[A-N]/C_0$  and  $[B-N]/C_0$  can be determined.

$$\frac{[A-N]}{C_0} = \frac{K_B r_A \overline{k_{p,B}} f_A}{K_A r_B \overline{k_{p,A}} f_B + K_B r_A \overline{k_{p,B}} f_A} \quad (27)$$

$$\frac{[B-N]}{C_0} = \frac{K_A r_B \overline{k_{p,A}} f_B}{K_A r_B \overline{k_{p,A}} f_B + K_B r_A \overline{k_{p,B}} f_A} \quad (28)$$

The average activation–deactivation equilibrium constant is then given by the following relationships.

$$\langle K \rangle = \frac{K_A K_B r_A \overline{k_{p,B}} f_A + K_B K_A r_B \overline{k_{p,A}} f_B}{K_A \overline{k_{p,A}} r_B f_B + K_B \overline{k_{p,B}} r_A f_A} \quad (29)$$

$$\langle K \rangle = \frac{\frac{r_A f_A}{k_{p,A}} + \frac{r_B f_B}{k_{p,B}}}{\frac{r_A f_A}{k_{p,A} K_A} + \frac{r_B f_B}{k_{p,B} K_B}} \quad (30)$$

$\langle k_p \rangle$  from the IPUE model has already been determined<sup>22–24</sup> (eq 31). It is then possible to give the  $\langle k_p \rangle \langle K \rangle$  product, which is an experimentally accessible parameter from the copolymerization kinetics (eq 32).

$$\langle k_p \rangle = \frac{r_A f_A^2 + 2f_A f_B + r_B f_B^2}{r_A \frac{f_A}{k_{p,A}} + r_B \frac{f_B}{k_{p,B}}} \quad (31)$$

$$\langle k_p \rangle \langle K \rangle = \frac{r_A f_A^2 + 2f_A f_B + r_B f_B^2}{\frac{r_A f_A}{k_{p,A} K_A} + \frac{r_B f_B}{k_{p,B} K_B}} \quad (32)$$

In ATRP, the equations for  $\langle K \rangle$  and  $\langle k_p \rangle \langle K \rangle$  (eqs 15, 17, 30, and 32) would be exactly the same. The only difference is in the way of writing the activation–deactivation equilibrium constants of eqs 2 and 3, where actually  $[N]$  should be replaced by  $[\text{deactivator}]/[\text{activator}]$ .

**3. Discussion about  $\langle K \rangle$  and  $\langle k_p \rangle \langle K \rangle$ .** The IPUE model better describes the copolymerization kinetics than the terminal model, whereas the latter allows only a good description of the copolymer composition.<sup>22–24</sup> Consequently,  $\langle K \rangle$  and  $\langle k_p \rangle \langle K \rangle$  are also better expressed with the IPUE model (eqs 30 and 32). With the recent development of the pulsed-laser polymerization to determine the absolute rate constants of (co)propagation, the  $r$  and  $s$  reactivity ratios have been now established for several comonomer couples,<sup>24</sup> which thus allows quite a good prediction of  $\langle K \rangle$  and  $\langle k_p \rangle \langle K \rangle$ . Only when the  $s$  values are not known can the TM equations be applied, to get an approximate trend.

The equation giving  $\langle K \rangle$  exhibits interesting features: it depends not only on the individual activation–deactivation equilibrium constants but also on the reactivity ratios and the homopropagation rate constants (i.e., on the cross-propagation rate constants expressed by the ratio of  $k_p$  over the corresponding monomer reactivity ratio). Additionally,  $\langle K \rangle$  is a function of the comonomer mixture composition. Consequently,  $\langle K \rangle$  changes with conversion throughout the copolymerization, in agreement with the continuous change in  $f_A$  and  $f_B$ . It appears also that a comonomer with a very high  $K$ , along with a high  $k_p$ , would not have a great influence on  $\langle K \rangle$ , over a broad composition range. This is, in particular, the point we want to illustrate in the following example.

## Experimental Application to the Nitroxide-Mediated Polymerization of Methyl Methacrylate

**1. Current Situation.** Nitroxide-mediated polymerization does not allow to control the family of methacrylic esters.<sup>25–28</sup> In the case of TEMPO (2,2,6,6-tetramethylpiperidinyl-1-oxy), the disproportionation reaction between the nitroxide and the growing radical, which yields an alkene chain-end along with a hydroxylamine, dominates over the reversible combination with

the nitroxide. It thus prevents the polymerization to reach large conversions and to produce nitroxide-terminated polymers.<sup>25–28</sup> Only copolymerizations with large amounts of styrene allowed to form copolymers with controlled molar mass and narrow molar mass distribution.<sup>29–31</sup> The polydispersity index, however, significantly increased when the proportion of methyl methacrylate was increased.

In contrast to TEMPO, the second generation of alicyclic nitroxides permits the control of a much broader range of monomers, such as the acrylates and substituted acrylamides.<sup>32–34</sup> This nitroxide family includes the *N-tert-butyl-N*-(1-diethylphosphono-2,2-dimethylpropyl) nitroxide, also called SG1 or DEPN,<sup>32,33</sup> and the 2,2,5-trimethyl-4-phenyl-3-azahexane 3-nitroxide (sometimes called TIPNO).<sup>34</sup> Nevertheless, they still do not allow a good control in the polymerization of methacrylic esters. The interesting point is that the disproportionation reaction between the nitroxide and the growing radical is absent.<sup>35</sup> The homopolymerization of methyl methacrylate remains, however, uncontrolled because of a too large activation–deactivation equilibrium constant<sup>35</sup> that leads to a high concentration of propagating macroradicals and hence favors their irreversible self-termination. Consequently, a complete disappearance of the active centers can occur within a very short time, and only very low limit conversions can be achieved. As shown by Benoit et al.,<sup>34</sup> the copolymerization of methyl methacrylate (MMA) with styrene (S) in the presence of TIPNO is, however, much better controlled than in the presence of TEMPO; this was demonstrated by the low polydispersity indexes observed for the copolymers, until 85 mol % of methyl methacrylate. The authors, however, did not provide any kinetic data (conversion vs time and average molar mass vs conversion) allowing to draw conclusion about the applicability of the controlled polymerization over a wide conversion range.

**2. Results and Discussion.** The conclusion of those various seminal works concerning the polymerization of methacrylic esters in the presence of an alicyclic nitroxide such as SG1 is that the best way to reach a high level of control would be to significantly reduce the activation–deactivation equilibrium constant. This would have the consequence of reducing the instantaneous concentration of propagating radicals and hence of decreasing the contribution of the irreversible termination. A possibility, purely based on the kinetic behavior, is to copolymerize methyl methacrylate with a small amount of an appropriate comonomer, in the presence of SG1. According to the eqs 15 and 30 giving  $\langle K \rangle$ , such comonomer should exhibit a much smaller activation–deactivation equilibrium constant than MMA along with a low cross-propagation rate constant ( $k_p$ /reactivity ratio). The latter point is important because a slow cross-propagation of the comonomer-based macroradical will ensure a longer lifetime, which is favorable to its efficient deactivation by the free nitroxide. In addition, the comonomer should also present a good control in the SG1-mediated polymerization; i.e.,  $K$  should not be too low. Styrene actually fulfills all the criteria, in particular at the optimal temperature of 90 °C, as illustrated by the kinetic and thermodynamic parameters given in Table 1. Unfortunately, the reactivity ratios are not available at 90 °C, and we considered here the data given at 57.2 °C in the literature,<sup>36</sup> assuming little temperature effect. Figure 1 gives the variation



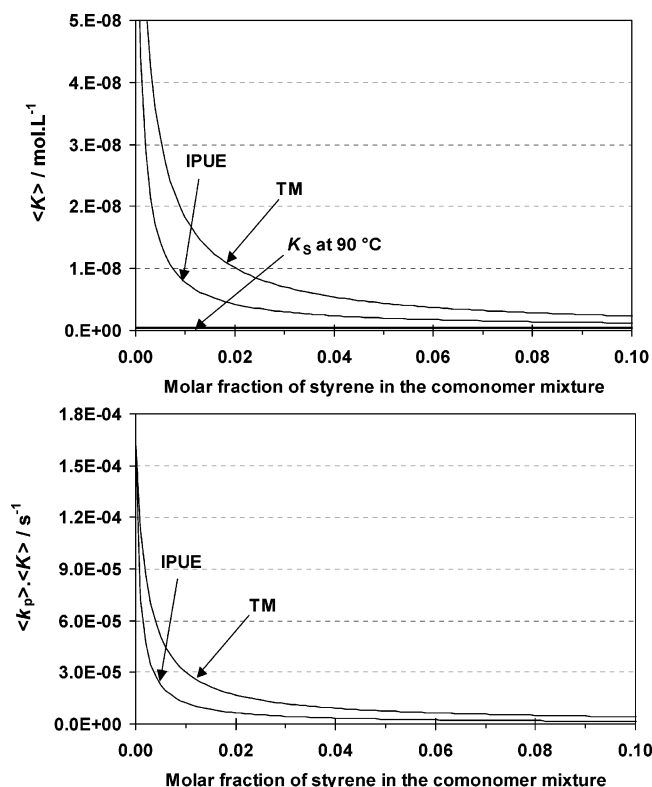
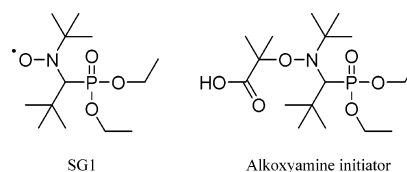
**Table 1. Kinetic Parameters for the SG1-Mediated Polymerization of Styrene (S) and Methyl Methacrylate (M)**

kinetic parameter		value	ref
$k_{p,S}$ at 90 °C (L mol <sup>-1</sup> s <sup>-1</sup> )	propagation rate constant of styrene	900	24
$k_{p,M}$ at 90 °C (L mol <sup>-1</sup> s <sup>-1</sup> )	propagation rate constant of methyl methacrylate	1640	24
$r_S$ (av value in the 20–60 °C range)	monomer reactivity ratio for styrene	0.4890	36
$r_M$ (av value in the 20–60 °C range)	monomer reactivity ratio for methyl methacrylate	0.4929	36
$s_S$ at 57.2 °C	radical reactivity ratio for styrene	0.3615	36
$s_M$ at 57.2 °C	radical reactivity ratio for methyl methacrylate	0.6014	36
$K_S$ at 90 °C (mol L <sup>-1</sup> )	activation-deactivation equilibrium constant for the SG1-mediated polymerization of styrene	$4 \times 10^{-10}$	33
$K_M$ at 90 °C (mol L <sup>-1</sup> )	activation-deactivation equilibrium constant for the SG1-mediated polymerization of methyl methacrylate	$1 \times 10^{-7}$	35

**Table 2. Predicted Values of the Average Activation–Deactivation Equilibrium Constant  $\langle K \rangle$  and of  $\langle k_p \rangle / \langle K \rangle$ , with  $\langle k_p \rangle$  the Average Propagation Rate Constant, for the Copolymerization of Methyl Methacrylate and Styrene at 90 °C Based on the Kinetic Parameters of Table 1, Using Either the Terminal Model (TM) or the Implicit Penultimate Unit Effect Model (IPUE)**

molar fraction of styrene in the comonomer mixture ( $f_S$ )	$\langle K \rangle$ (mol L <sup>-1</sup> )		$\langle k_p \rangle / \langle K \rangle$ (s <sup>-1</sup> )	
	TM (from eq 15)	IPUE (from eq 30)	TM (from eq 17)	IPUE (from eq 32)
0	$1.0 \times 10^{-7}$	$1.0 \times 10^{-7}$	$1.6 \times 10^{-4}$	$1.6 \times 10^{-4}$
0.025	$8.3 \times 10^{-9}$	$3.5 \times 10^{-9}$	$1.4 \times 10^{-5}$	$5.4 \times 10^{-6}$
0.05	$4.4 \times 10^{-9}$	$2.0 \times 10^{-9}$	$7.6 \times 10^{-6}$	$2.9 \times 10^{-6}$
0.10	$2.3 \times 10^{-9}$	$1.2 \times 10^{-9}$	$4.2 \times 10^{-6}$	$1.6 \times 10^{-6}$
1	$4.0 \times 10^{-10}$	$4.0 \times 10^{-10}$	$3.6 \times 10^{-7}$	$3.6 \times 10^{-7}$

of  $\langle K \rangle$  in the copolymerization of methyl methacrylate with increasing proportions of styrene from 0 to 10 mol %. Only below 3–4 mol % of styrene is  $\langle K \rangle$  increasing very significantly. Above this fraction, the value of  $\langle K \rangle$  is close to that found for the styrene–SG1 system (Table 2). Consequently, at best, the system might exhibit the same quality of control as that found in the SG1-mediated homopolymerization of styrene. Another mono-

**Scheme 1. Structure of the SG1 Nitroxide Deactivator and of the SG1-Based Alkoxyamine Initiator Used in This Work****Figure 1.** Predicted values of the average activation–deactivation equilibrium constant  $\langle K \rangle$  and of  $\langle k_p \rangle / \langle K \rangle$ , with  $\langle k_p \rangle$  the average propagation rate constant, as a function of the molar fraction of styrene in the comonomer mixture, for the copolymerization of methyl methacrylate and styrene at 90 °C based on the kinetic parameters of Table 1, using either the terminal model (TM) or the implicit penultimate unit effect model (IPUE).

mer with a lower  $K$  than styrene might be used instead. Considering only  $K$ , *n*-butyl acrylate would be a good choice since  $K = 2 \times 10^{-10}$  at 120 °C.<sup>33</sup> However, the very high  $k_p$  value<sup>24,37</sup> does not allow a sufficient decrease of  $\langle K \rangle$ , which remains above  $5 \times 10^{-9}$  for *n*-butyl acrylate contents below 75 mol %. For such comonomer, the cross-propagation of the *n*-butyl acrylate-terminated macroradical is much faster than its deactivation by SG1.

We first intended to check the quality of control in the copolymerization of MMA with various ratios of styrene, from 0 to 8.8 mol %, expecting to find a similar control as in the homopolymerization of styrene for the largest ratios. To reduce the rate of irreversible termination from the early polymerization stages, we decided to introduce 10 mol % of free SG1, based on the initiator, at the beginning of the polymerization. To optimize the control, the polymerizations were performed at 90 °C with an alkoxyamine initiator able to dissociate at a sufficiently low temperature (owing to the presence of a tertiary carbon radical attached to the nitroxide; see Scheme 1 and the experimental part)<sup>38</sup> to induce a fast initiation process. The results are shown in Figure 2 for experiments 1–4 summarized in Table 3. In the absence of styrene, the homopolymerization of MMA stopped at low conversion within a very short time, indicating the prevalence of the irreversible termination. The formed poly(methyl methacrylate) had a number-average molar mass in rather good agreement with the theoretical value, but a high polydispersity index (1.8). With the addition of 2.1 mol % of styrene, the situation significantly improved, but a limit conversion of  $\approx 50\%$  was reached within 1 h, indicating the strong decrease of the propagating radicals. The quality of control was also improved, but the polydispersity indexes increased

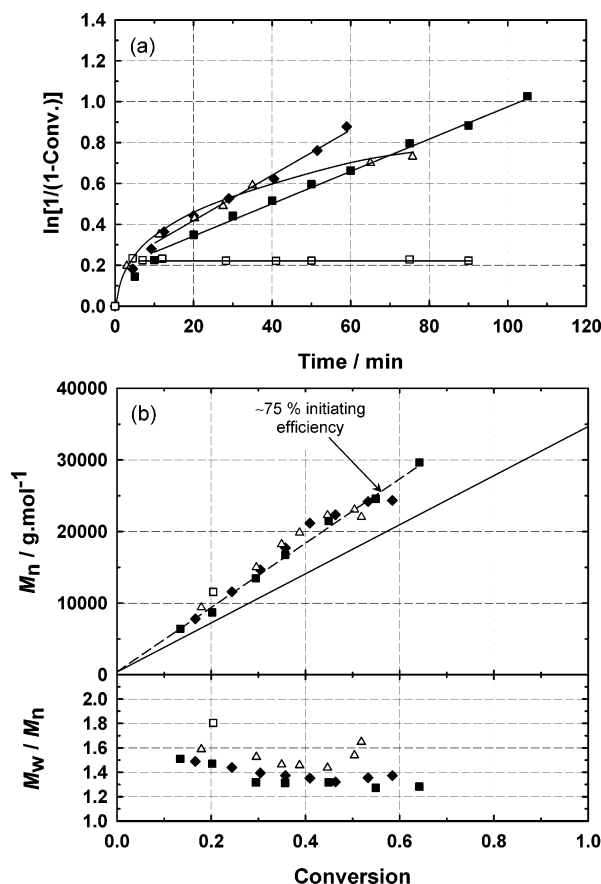


**Figure 2.** Bulk polymerizations of methyl methacrylate at 90 °C, in the presence of  $2.73 \times 10^{-2}$  mol L $^{-1}$  of alkoxyamine initiator, 10 mol % of added free SG1 based on the initiator, and various initial molar fractions of styrene ( $f_{S0}$ ) (see Table 3): ■, experiment 1 ( $f_{S0} = 0.088$ ); ♦, experiment 2 ( $f_{S0} = 0.044$ ); △, experiment 3 ( $f_{S0} = 0.021$ ); □, experiment 4 ( $f_{S0} = 0$ ). (a)  $\ln[1/(1 - \text{conv})]$  vs time (conv = overall conversion); (b) number-average molar mass,  $M_n$ , and polydispersity index,  $M_w/M_n$ , vs conversion; the full line represents the theoretical  $M_n$ , whereas the dotted line is the linear regression for the experimental data.

with conversion, beyond 40% conversion. In contrast, at and above 4.4 mol % of styrene, the polymerization exhibited all the features of a well-defined system, allowing to reach high conversions while keeping a good control over the molar mass and molar mass distribution. The experimental  $M_n$ 's increased with conversion, in good agreement with the predicted values; they were, however, systematically above the theoretical line, indicating an incomplete initiation ( $\approx 75\%$  initiating efficiency; see Figure 2) due to irreversible termination of primary radicals and/or oligoradicals, leading to short dead chains not taken into consideration in the SEC chromatograms (care should however be taken in quantifying the initiating efficiency owing to the experimen-

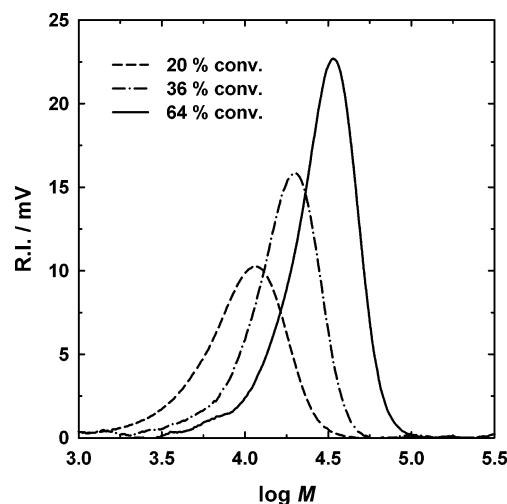


**Figure 3.** Size exclusion chromatograms recorded at various conversions for the bulk copolymerization of methyl methacrylate (8.48 mol L $^{-1}$ ) and styrene (0.82 mol L $^{-1}$ ;  $f_{S0} = 0.088$ ) at 90 °C, carried out in the presence of  $2.73 \times 10^{-2}$  mol L $^{-1}$  of alkoxyamine initiator and 10 mol % of added free SG1 based on the initiator (experiment 1) (see Table 3).

tal error of the SEC measurements; see Experimental Part). Such a result would indicate that the added 10 mol % (based on the initiator) of free SG1 was not sufficient to significantly reduce the early irreversible terminations. Nevertheless, the polydispersity indexes continuously decreased throughout the polymerization to reach values as low as 1.2–1.3. Moreover, the polymerization rate slightly decreased with the increase in the proportion of styrene, in agreement with the small decrease in  $\langle k_p \rangle / \langle K \rangle$  (Table 2). Figure 3 shows the SEC chromatograms at increasing conversions for the copolymerization with 8.8 mol % of styrene (experiment 1): the complete shift of the RI traces toward higher molar masses proves that the polymerization proceeded via an activation–deactivation mechanism that allowed all the chains to grow simultaneously. The tailing on the low molar mass side, however, might be reasonably assigned to the contribution of irreversible terminations. It should be mentioned that, based on the reactivity ratios, at low molar fraction, styrene is consumed faster than methyl methacrylate ( $^1\text{H}$  NMR gave 4 mol % of styrene in the copolymer isolated at 52% conversion for the experiment with  $f_{S0} = 0.021$ ; 7 mol % of styrene at 58% conversion for  $f_{S0} = 0.044$ ; and 12 mol % of styrene at 64% conversion for  $f_{S0} = 0.088$ ), leading to a continuous decrease of  $f_S$  throughout the copolymerization, and hence a continuous increase in  $\langle K \rangle$ . Consequently, the quality of control should decline with conversion, leading to enhanced irreversible termination. Nevertheless, this trend should be counterbalanced by a decrease of the rate constant of termination with the increase in macroradical chain length.<sup>39</sup>

**Table 3.** Experimental Conditions for the SG1-Mediated Bulk (Co)polymerizations of Methyl Methacrylate (M) and Styrene (S) at 90 °C

expt	[M] (mol L $^{-1}$ )	[S] (mol L $^{-1}$ )	initial molar fraction of styrene ( $f_{S0}$ )	initial concn of alkoxyamine (mol L $^{-1}$ )	initial concn of SG1 nitroxide <sup>a</sup> (mol L $^{-1}$ )
1	8.48	0.82	0.088	$2.73 \times 10^{-2}$	$2.74 \times 10^{-3}$
2	8.92	0.41	0.044	$2.72 \times 10^{-2}$	$2.75 \times 10^{-3}$
3	9.14	0.20	0.021	$2.73 \times 10^{-2}$	$2.74 \times 10^{-3}$
4	9.36	0	0	$2.73 \times 10^{-2}$	$2.74 \times 10^{-3}$
5	8.49	0.82	0.088	$5.46 \times 10^{-2}$	$5.45 \times 10^{-3}$
6	8.49	0.82	0.088	$1.37 \times 10^{-2}$	$1.36 \times 10^{-3}$

<sup>a</sup> [SG1]/[alkoxyamine initiator]<sub>0</sub> = 0.10; structure of the SG1 nitroxide and of the alkoxyamine is shown in Scheme 1.

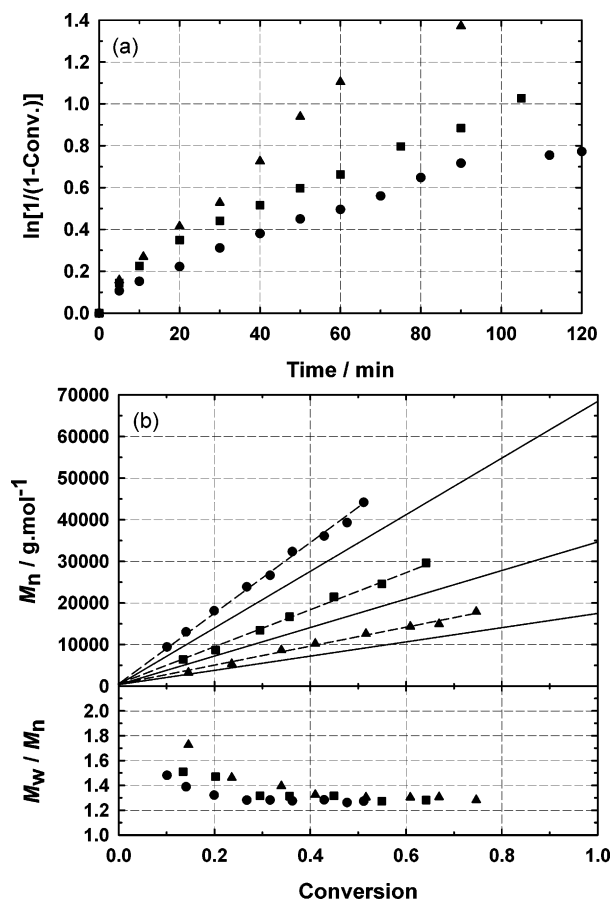


**Figure 4.** Bulk copolymerizations of methyl methacrylate and styrene ( $f_{S0} = 0.088$ ) at 90 °C in the presence of 10 mol % of added free SG1 based on the initiator, with various initiator concentrations (see Table 3): ●, experiment 6 ( $1.37 \times 10^{-2}$  mol L $^{-1}$ ); ■, experiment 1 ( $2.73 \times 10^{-2}$  mol L $^{-1}$ ); ▲, experiment 5 ( $5.46 \times 10^{-2}$  mol L $^{-1}$ ). (a)  $\ln[1/(1 - \text{conv})]$  vs time (conv = overall conversion); (b) number-average molar mass,  $M_n$ , and polydispersity index,  $M_w/M_n$ , vs conversion; the full lines represent the theoretical  $M_n$ 's, whereas the dotted lines are the linear regressions for the experimental data.

The alkoxyamine initiator concentration was then varied for experiments 1, 5, and 6 with 8.8 mol % of styrene based on the monomers and 10 mol % of free SG1 based on the alkoxyamine to target different molar masses. In all three experiments, well-defined polymers were obtained, with a high level of control (Figure 4):  $M_n$  followed the predicted values, even though they remained slightly above, and the polydispersity indexes were as low as 1.3 at large conversions. Unexpectedly, the polymerization rate was different for all three experiments despite a similar  $C_0/[N]_0$  initial ratio. This result is in agreement with the previously mentioned indication that the added free SG1 was not in sufficient concentration to avoid the existence of irreversible terminations. New free SG1 is released in the early stage of the polymerization, in larger proportion when the initial concentration of alkoxyamine is lower, leading to a decreased polymerization rate when  $C_0$  is decreased. This trend is in good agreement with the equations describing the persistent radical effect.<sup>21</sup> The existence of early termination reactions is also confirmed by the incomplete initiator efficiency (experimental  $M_n$ 's above the theoretical line; see Figure 4).

## Conclusion

The average activation–deactivation equilibrium constant,  $\langle K \rangle$ , was determined on a theoretical basis for controlled free-radical copolymerization operating via a reversible termination mechanism, using the terminal model for the activation–deactivation equilibrium and the terminal model or the implicit penultimate unit effect model for the propagation reaction. The form of the equation shows that  $\langle K \rangle$  remains close to the lowest activation–deactivation equilibrium constant in a copolymerization system where a monomer with a very large  $K$  is copolymerized with a monomer with a low  $K$ , even if the latter is added in very small proportion. The reactivity ratios and the homopropagation rate constants have also a nonnegligible influence (direct effect of the cross-propagation rate). Consequently, the addition of a small fraction of an appropriate comonomer can be performed in order to enhance the control of a monomer that exhibits a too high  $K$ , detrimental to a good control. The method was indeed successfully applied to the nitroxide-mediated polymerization of methyl methacrylate at 90 °C, with SG1 as a nitroxide. By adding 4.4 or 8.8 mol % of styrene, the polymerization could be carried out to large conversions, while exhibiting all the features of a controlled system. In this copolymerization system, the reactivity ratios and the composition parameter  $f_S$  are such that the chains contain isolate styrene subunits. The existence of styrene-terminated macroradicals favors the deactivation reaction, which would not otherwise efficiently take place with a methyl methacrylate terminal unit.

A further step of this work is to analyze the chain ends (overall alkoxyamine end-functionality and nature of the terminal monomer unit attached to the SG1) in order to draw conclusions about the true livingness of the system. Nevertheless, the method allows to build controlled methacrylic ester-rich macromolecular architectures via SG1-mediated free-radical polymerization. The important point is that it enables high conversions to be reached, which represents a very important breakthrough for the technique.

## Experimental Part

**1. Materials.** Methyl methacrylate (MMA or M, Aldrich, 99%) and styrene (S, Aldrich, 99%) were distilled under reduced pressure before use. The SG1-based alkoxyamine initiator with the 2-(hydroxycarbonyl)prop-2-yl radical<sup>38</sup> (Bloc-Buider, Arkema, 99%, see Scheme 1) and the *N*-tert-butyl-*N*-(1-diethylphosphono-2,2-dimethylpropyl) nitroxide (SG1, 86%, see Scheme 1) were kindly supplied by Arkema.

**2. Bulk Polymerizations.** In a typical experiment (experiment 1, see Table 3), a mixture of methyl methacrylate (80.0 g, 0.80 mol), styrene (8.0 g, 0.77 mol), and SG1 (0.076 g, 0.26 mmol) was deoxygenated by nitrogen bubbling for 20 min at room temperature. The alkoxyamine initiator (0.980 g, 2.57 mmol) was added, and nitrogen bubbling was carried out for 10 min. The mixture was then introduced into a 250 mL three-neck round-bottom flask heated at 90 °C, immersed in a thermostated oil bath, and equipped with a reflux condenser, a nitrogen inlet, and a thermometer. The time zero of the reaction was triggered when temperature in the reactor reached 85 °C. Samples of about 5 mL were periodically withdrawn to follow the monomer conversion by gravimetry; they were dried in a ventilated oven thermostated at 70 °C under vacuum, until constant weight. Conditions for the various bulk polymerizations are summarized in Table 3.

**3. Analytical Techniques.** Size exclusion chromatography (SEC) was performed at 40 °C with two columns (PSS SDV, linear MU, 8 mm  $\times$  300 mm; bead diameter: 5  $\mu$ m; separation



limits:  $400\text{--}2 \times 10^6 \text{ g mol}^{-1}$ ). The eluent was tetrahydrofuran at a flow rate of  $1 \text{ mL min}^{-1}$ . A differential refractive index (RI) detector (LDC Analytical refractoMonitor IV) was used, and molar mass distributions were derived from a calibration curve based on polystyrene (PS) standards from Polymer Standards Service. The polystyrene calibration is not appropriate for poly(methyl methacrylate) (PMMA) samples. Thus, the  $M_n$  values obtained from polystyrene conventional calibration were converted using the Mark–Houwink–Sakurada (MHS) relationship between PS and PMMA with MHS parameters determined at  $35^\circ\text{C}$ :  $K_{\text{PS}} = 15.8 \times 10^{-5} \text{ dL g}^{-1}$ ,  $\alpha_{\text{PS}} = 0.704$ ,  $K_{\text{PMMA}} = 12.2 \times 10^{-5} \text{ dL g}^{-1}$ , and  $\alpha_{\text{PMMA}} = 0.69$ .<sup>40</sup> In all the figures representing the experimental  $M_n$  as a function of monomer conversion, the displayed full line corresponds to the theoretical evolution of  $M_n$  calculated by

$$M_n = \text{MW(alkoxyamine initiator)} + \frac{\text{initial mass of monomers}}{\text{initial mol number of alkoxyamine}} \times \text{conversion}$$

The final copolymer compositions were analyzed by  $^1\text{H}$  NMR spectroscopy (250 MHz) in  $\text{CDCl}_3$  solution, at  $25^\circ\text{C}$ , in 5 mm tubes, using a AC250 Bruker spectrometer.

**Acknowledgment.** The authors thank Stéphanie Magnet and Jean-Luc Couturier from ARKEMA for fruitful discussions and for kindly providing the SG1 and the alkoxyamine.

## References and Notes

- (1) (a) *Controlled Radical Polymerization*; Matyjaszewski, K., Ed.; ACS Symp. Ser. **1998**, 685. (b) *Controlled/Living Radical Polymerization: Progress in ATRP, NMP, and RAFT*; Matyjaszewski, K., Ed.; ACS Symp. Ser. **2000**, 768. (c) *Advances in Controlled/Living Radical Polymerization*; Matyjaszewski, K., Ed.; ACS Symp. Ser. **2003**, 854.
- (2) Hawker, C. J.; Bosman, A. W.; Harth, E. *Chem. Rev.* **2001**, *101*, 3661–3688.
- (3) Matyjaszewski, K.; Xia, J. *Chem. Rev.* **2001**, *101*, 2921–2990.
- (4) Kamigaito, M.; Ando, T.; Sawamoto, M. *Chem. Rev.* **2001**, *101*, 3689–3745.
- (5) Madruga, E. L. *Prog. Polym. Sci.* **2002**, *27*, 1879–1924 and references therein.
- (6) Farcet, C.; Charleux, B.; Pirri, R. *Macromol. Symp.* **2002**, *182*, 249–260.
- (7) Couvreur, L.; Charleux, B.; Guerret, O.; Magnet, S. *Macromol. Chem. Phys.* **2003**, *204*, 2055–2063.
- (8) Gray, M. K.; Zhou, H.; Nguyen, S. T. Torkelson, J. M. *Macromolecules* **2004**, *37*, 5586–5595.
- (9) Gray, M. K.; Zhou, H.; Nguyen, S. T. Torkelson, J. M. *Polymer* **2004**, *45*, 4777–4786.
- (10) Ziegler, M. J.; Matyjaszewski, K. *Macromolecules* **2001**, *34*, 415–424.
- (11) Matyjaszewski, K.; Ziegler, M. J.; Arehart, S. V.; Greszta, D.; Pakula, T. *J. Phys. Org. Chem.* **2000**, *13*, 775–786.
- (12) Butz, S.; Baethge, H.; Schmidt-Naake, G. *Angew. Macromol. Chem.* **1999**, *270*, 42–48.
- (13) Heuts, J. P. A.; Davis, T. P. *Macromol. Rapid Commun.* **1998**, *19*, 371–375.
- (14) Arehart, S. V.; Matyjaszewski, K. *Macromolecules* **1999**, *32*, 2221–2231.
- (15) Zaremski, M. Y.; Plutalova, A. V.; Lachinov, M. B.; Golubev, V. B. *Macromolecules* **2000**, *33*, 4365–4372.
- (16) Bisht, H. S.; Ray, S. S.; Pandey, D.; Sharma, C. D.; Chatterjee, A. K. *J. Polym. Sci., Part A: Polym. Chem.* **2002**, *40*, 1818–1830.
- (17) Skeist, I. *J. Am. Chem. Soc.* **1946**, *68*, 1781–1784.
- (18) Klumperman, B.; Chambard, G.; Brinkhuis, R. H. G. *ACS Symp. Ser.* **2003**, *854*, 180–192.
- (19) Matyjaszewski, K. *Macromolecules* **2002**, *35*, 6773–6781.
- (20) Fischer, H. *Chem. Rev.* **2001**, *101*, 3581–3610.
- (21) Goto, A.; Fukuda, T. *Prog. Polym. Sci.* **2004**, *29*, 329–385.
- (22) Fukuda, T.; Ma, Y.-D.; Inagaki, H. *Macromolecules* **1985**, *18*, 17–26.
- (23) Coote, M. L.; Davis, T. P. *Prog. Polym. Sci.* **1999**, *24*, 1217–1251.
- (24) Beuermann, S.; Buback, M. *Prog. Polym. Sci.* **2002**, *27*, 191–254.
- (25) Moad, G.; Anderson, A. G.; Ercole, F.; Johnson, C. H. J.; Krstina, J.; Moad, C. L.; Rizzardo, E.; Spurling, T. H.; Thang, S. H. *ACS Symp. Ser.* **1998**, *685*, 332–360.
- (26) Burguière, C.; Dourges, M.-A.; Charleux, B.; Vairon, J.-P. *Macromolecules* **1999**, *32*, 3883–3890.
- (27) Ananchenko, G. S.; Fischer, H. *J. Polym. Sci., Part A: Polym. Chem.* **2001**, *39*, 3604–3621.
- (28) Souaille, M.; Fischer, H. *Macromolecules* **2001**, *34*, 2830–2838.
- (29) Hawker, C. J.; Elce, E.; Dao, J.; Volksen, W.; Russell, T. P.; Barclay, G. G. *Macromolecules* **1996**, *29*, 2686–2688.
- (30) Butz, S.; Baethge, H.; Schmidt-Naake, G. *Macromol. Rapid Commun.* **1997**, *18*, 1049–1055.
- (31) Miura, Y.; Nakamura, N.; Taniguchi, I.; Ichikawa, A. *Polymer* **2003**, *44*, 3461–3467.
- (32) Grimaldi, S.; Finet, J. P.; Le Moigne, F.; Zeghdou, A.; Tordo, P.; Benoit, D.; Fontanille, M.; Gnanou, Y. *Macromolecules* **2000**, *33*, 1141–1147.
- (33) Benoit, D.; Grimaldi, S.; Robin, S.; Finet, J. P.; Tordo, P.; Gnanou, Y. *J. Am. Chem. Soc.* **2000**, *122*, 5929–5939.
- (34) Benoit, D.; Chaplinski, V.; Braslau, R.; Hawker, C. J. *J. Am. Chem. Soc.* **1999**, *121*, 3904–3920.
- (35) Ananchenko, G. S.; Souaille, M.; Fischer, H.; Le Mercier, C.; Tordo, P. *J. Polym. Sci., Part A: Polym. Chem.* **2002**, *40*, 3264–3283.
- (36) Coote, M. L.; Johnston, L. P. M.; Davis, M. P. *Macromolecules* **1997**, *30*, 8191–8204.
- (37) Asua, J. M.; Beuermann, S.; Buback, M.; Castignolles, P.; Charleux, B.; Gilbert, R. G.; Hutchinson, R. A.; Leiza, J. R.; Nikitin, A. N.; Vairon, J.-P.; van Herk, A. M. *Macromol. Chem. Phys.* **2004**, *205*, 2151–2160.
- (38) Couturier, J. L.; Guerret, O.; Bertin, D.; Gimes, D.; Marque, S.; Tordo, P.; Chauvin, F.; Dufils, P. E. WO 2004/014926.
- (39) Buback, M.; Egorov, M.; Gilbert, R. G.; Kaminsky, V.; Olaj, O. F.; Russell, G. T.; Vana, P.; Zifferer, G. *Macromol. Chem. Phys.* **2002**, *203*, 2570–2582.
- (40) Mori, S.; Barth, H. G. *Size Exclusion Chromatography*; Springer-Verlag: Berlin, 1999; p 201.

MA050087E